Tapping Mode Atomic Force Microscopy of Hyaluronan: Extended and Intramolecularly Interacting Chains

Mary K. Cowman,* Min Li,* and Endre A. Balazs#
*Department of Chemical Engineering, Chemistry, and Materials Science and Herman F. Mark Polymer Research Institute, Polytechnic University, Brooklyn, New York 11201, and #Biomatrix, Inc., Ridgefield, New Jersey 07657 USA

ABSTRACT The extracellular matrix polysaccharide hyaluronan has been examined by tapping mode atomic force microscopy. High molecular weight hyaluronan was deposited on mica from dilute aqueous solution and imaged in air. Long unbranched chains could be observed and were found to be compatible with the known covalent structure of hyaluronan. In addition, chains with evidence of intramolecular association were observed. In the simplest cases, the association took the form of loops stabilized by antiparallel double-stranded (probably double-helical) segments. In other cases, the polarity of the associated regions could not be determined. Extensive intramolecular association in long hyaluronan chains resulted in a fenestrated structure of the same type as that formed by intermolecular association at higher concentrations.

INTRODUCTION

The extracellular matrix polysaccharide hyaluronan (HA) is a high molecular weight linear polymer with the repeating disaccharide structure poly[(1→3)-β-D-GlcNAc-(1→4)-β-D-GlcA-] (Meyer, 1958). HA is responsible for the elastoviscosity of the joint synovial fluid and eye vitreus (Balazs, 1968; Balazs and Denlinger, 1985), participates in the control of tissue hydration and water transport, and serves as the structural backbone of cartilage proteoglycan assemblies. Via specific cell surface receptor proteins, HA affects numerous biological processes, such as development, tumor metastasis, and inflammation (Laurent et al., 1996).

In dilute aqueous solution at physiological pH and ionic strength, HA behaves as a random coil with a large hydrodynamic volume. As a result of the chain stiffness and high molecular weight of HA (generally 2×10^6 to 6×10^6), the coils touch and begin to entangle (i.e., reach the coil overlap point) at a low concentration. For example, HA with a molecular weight of 3×10^6 begins to entangle at a concentration of ~1 mg/ml (Morris et al., 1980; Yanaki and Yamaguchi, 1990; Yu et al., 1992; Fouissac et al., 1993). To study the structural properties of isolated HA chains, the solution concentration should be much below this value.

HA has also been shown to self-associate in physiological NaCl solution (Sheehan et al., 1983; Turner et al., 1988; Cowman et al., 1998). Both intramolecular and intermolecular self-association of HA can strongly affect solution rheology, water retention, and water transport. It is also likely that HA association alters the thermodynamics and kinetics of interaction with binding proteins.

The mode of association between HA strands has been the subject of considerable investigation. X-ray fiber diffraction data for the sodium salt of HA show single helices, packed in an antiparallel manner (Guss et al., 1975; Sheehan and Atkins, 1983). A double-helical structure, with antiparallel chains, was observed under unusual counterion conditions (e.g, Rb^+, Cs^+, mixed K^+, H^+) (Sheehan et al., 1977; Arnott et al., 1983). Evidence for the existence in physiological solution of a hairpin turn structure, stabilized by interaction between two antiparallel chain segments, was provided by light-scattering and spectroscopic studies of HA fragments (Turner et al., 1988).

Imaging HA by electron microscopy (EM) has provided a picture of extensively interacting networks (Scott et al., 1991; Brewton and Mayne, 1992). The network structure arises from intermittent formation of junctions containing two or more chains. EM studies of HA also support the existence of loops stabilized by double-stranded regions (Scott et al., 1990), but image resolution has been insufficient to prove interaction along the length of a loop stem. Atomic force microscopy (AFM) has the necessary resolution to establish interaction modes and provides a three-dimensional image to establish structural details. Phillips and co-workers (Gunning et al., 1996) provided the first AFM data for HA. Network formation was predominant in the images, which were obtained for HA samples dried on a mica surface and overlaid with organic solvent. We have also observed networks of HA chains under more hydrated conditions, by using tapping mode AFM (TMAFM) in air, where a thin layer of adsorbed gases and water covers the mica surface (Cowman et al., 1998). In addition, we have used TMAFM to visualize individual chains of HA at high resolution.

In the present study, we have continued and extended our earlier TMAFM investigations of HA structure. These studies are part of a continuing effort to elucidate details of the structure and stabilization of self-association in HA.

MATERIALS AND METHODS

Hyaluronan (HA) isolated from rooster combs (Healon) was obtained as a 1% (w/v) solution in physiological buffered saline (145 mM NaCl, 0.34

Received for publication 23 March 1998 and in final form 25 June 1998.
Address reprint requests to Dr. Mary K. Cowman, Department of Chemical Engineering, Chemistry, and Materials Science, Polytechnic University, Six Metrotech Center, Brooklyn, NY 11201. Tel.: 718-260-3054; Fax: 718-260-3125; E-mail: mcowman@duke.poly.edu.

0006-3495/98/10/2030/08 $2.00

mM NaH_2PO_4, 1.5 mM Na_2HPO_4) from Pharmacia and Upjohn (Piscataway, NJ). Its weight-average molecular weight was estimated by agarose gel electrophoresis (Lee and Cowman, 1994) as 4.2×10^6. Unless otherwise noted, all images were obtained with this sample. HA isolated from *Streptococcus zooepidemicus* was obtained as a dry powder from Sigma Chemical Co. (St. Louis, MO). Its weight-average molecular weight was estimated by agarose gel electrophoresis as 2.2×10^6 and also determined by low-angle laser light scattering as 2.2×10^6. For AFM studies, the rooster comb HA was first diluted with distilled water to an HA concentration of 100 μg/ml. Portions of this stock solution were mixed with 100 mM $MgCl_2$ and water to yield final HA concentrations of 1–4 μg/ml in 10 mM $MgCl_2$. The bacterial HA was initially dissolved in physiological buffered saline at an HA concentration of 500 μg/ml. Portions of this stock solution were mixed with 100 mM $MgCl_2$ and water to yield a final HA concentration of 5 μg/ml in 10 mM $MgCl_2$.

A 4-μl drop of dilute (1–5 μg/ml) HA solution was applied to freshly cleaved mica. After a waiting time of 1–2 min, the surface was rinsed with either 2×200 μl or 3×100 μl of distilled water and then dried for approximately 1 min under a gentle stream of dry N_2 until the surface appeared dry. The mica surface was used immediately for AFM studies. The AFM instrument was a Nanoscope IIIa Multimode scanning probe microscope, equipped with a type EV scanner (Digital Instruments, Santa Barbara, CA). Images were obtained at ambient temperature and humidity. The tapping mode was employed, using etched silicon cantilever probes of 125 μm nominal length, at a drive frequency of ~300 kHz. We generally use a root-mean-square voltage of approximately 2.5–3.0 V and adjust the set-point voltage for optimal image quality, which is generally ~1 V less than the root-mean-square voltage. Both height and phase data were recorded at a scan rate of 1–2 Hz and stored in either 256- × 256- or 512- × 512-pixel format. Images were processed using the Nanoscope version 4.22 software. For images to be used in measuring heights, the only image processing was zero order flattening. For any given image, the height was analyzed in at least three distinct regions of the structure being analyzed. For optimal image quality in visualizing chain features (and therefore for use in figures), flattening of first order was used unless otherwise stated. The only other image adjustments were setting the image height range, color contrast, and color offset for best appearance of structural details.

RESULTS

TMAFM imaging of HA after deposition on mica from physiological saline solution containing hyaluronan at a concentration of approximately 100 μg/ml yielded a network of overlapping and interacting strands (Cowman et al., 1998). As solutions of high molecular weight (~10^6) HA at the same concentration are below the coil overlap point, the intermolecular network is formed on the surface of the mica. Similar observations had been made by electron microscopy (Scott et al., 1990, 1991; Brewton and Mayne, 1992) and AFM (Gunning et al., 1996) on dehydrated samples. The artifactual network is a useful illustration of the strong tendency of HA to self-associate as the local concentration increases.

We have also previously reported the successful TMAFM imaging of HA as an isolated extended chain (Cowman et al., 1998). To do so, we found it necessary to use extremely dilute HA solutions (1–5 μg/ml). It was also necessary to promote the adhesion of HA to the mica surface by adding a low concentration (10 mM) of $MgCl_2$ to the HA solution (as is often done in imaging DNA). Excess ions are removed in a washing step, and the surface was dried under nitrogen flow. Under these conditions, the air-exposed mica surface retains a thin layer (perhaps a few nanometers thick) of adsorbed gases and water. The HA is therefore in a more hydrated state under these conditions than is the case for electron microscopy studies or AFM under organic solvents. Adhesive forces between the tip and water on the surface makes contact AFM imaging in air difficult. Tapping mode AFM allows the tip to drive through the water layer and obtain high-quality surface images. Tapping mode also allows the simultaneous acquisition of topographic (height) information and phase information, the latter being a function of factors such as surface adhesion and elasticity. The phase image is derived from the phase lag of the cantilever oscillation relative to the signal sent to the piezoelectric driver, which induces the tip to oscillate at its resonant frequency. Because the phase data accentuate edges, it is occasionally useful in resolving fine details of structure not seen in the height data. Using the above-described procedures in the present study, we were able to obtain images of individual HA chains illustrating a variety of structural forms. These forms illustrate the manner in which HA self-associates.

Isolated chains without intramolecular self-association

Fig. 1 shows an isolated and extended HA molecule, with an apparent loop near one end. Both the height and phase images are shown, because a surface artifact caused the height image to be degraded, whereas the phase image allowed the complete chain to be better observed. The chain length is estimated to be ~6.5 μm. If that length is assumed to correspond to an extended HA conformation, for which the projection of the disaccharide repeat along the chain axis is expected to be 0.8–1.0 nm, then the chain would contain 6500–8125 disaccharides, corresponding to a molecular weight of 2.6×10^6 to 3.3×10^6. In 18 images of different HA molecules from the same sample, for which the chain contour could be followed with reasonable confidence, the length varied from 1.0 to 6.8 μm. The number-average length was 3.0 μm, and the weight-average length was 4.1 μm. The weight-average length corresponds to a weight-average molecular weight of 1.6×10^6 to 2.0×10^6 if the chains are completely extended. The actual weight-average molecular weight of the rooster comb HA sample employed in these studies was estimated by gel electrophoresis as 4.2×10^6. The discrepancy probably indicates only that long HA chains are difficult to image in the extended form without chain collapse or association and that our 18-image sample is much too small for statistical analysis.

The height of isolated HA molecules was analyzed in a number of spots on each image. We found that the height was approximately 0.6 ± 0.1 nm if the measurements were made from images with a data point density in the x-y plane of at least 0.5 points/nm. Images with lower data density (0.1–0.4 points/nm) gave a lower height (0.4 ± 0.1 nm). We speculate that this simply reflects the reduced likelihood that data were obtained from the highest point in the chain

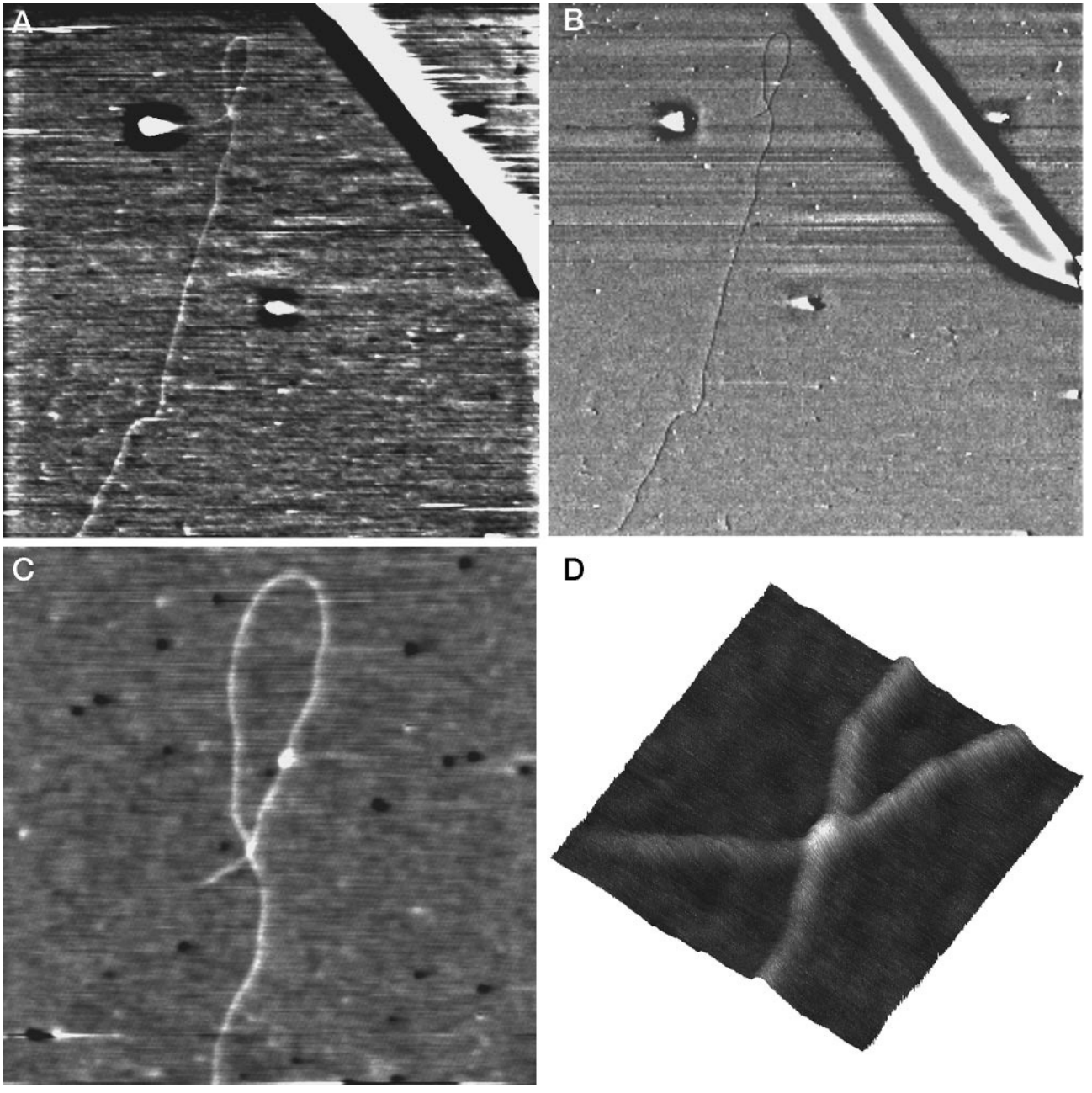

FIGURE 1 TMAFM images of an extended HA chain near an artifact on the mica surface. (*A*) Height image, 5.1 μm $\times$ 5.1 μm (contrast enhanced), with gray scale covering 1.5 nm in height; (*B*) Phase image, 5.1 μm $\times$ 5.1 μm, with gray scale covering 6° phase difference; (*C*) Height image of loop region, 1.5 μm $\times$ 1.5 μm, with gray scale covering 1.5 nm in height; (*D*) Surface plot of the crossover point of the loop structure, 300 nm $\times$ 300 nm, with 2.5-nm height scale.

cross section, recalling that the chain diameter is presumed equal to the sub-nanometer height. The height of 0.6 nm is consistent with the expected diameter of a single HA chain.

The chain in Fig. 1 *A* forms a loop near the top of the image field, which is shown in more detail in Fig. 1 *C*. The point at which the chain crosses itself is shown in a 300-nm $\times$ 300-nm $\times$ 2.5-nm surface view in Fig. 1 *D*. The chain segments do not appear to interact over an extended length but merely cross. The height at the crossover point in this image is 1.1 $\pm$ 0.1 nm, which is close to twice the average height of an isolated HA chain.

Isolated chains with intramolecular association

HA chains with apparent self-association were more commonly observed than were extended chains. Fig. 2 *A* shows an HA chain with an apparent length of $\sim$6.8 μm and a height of $\sim$0.6 $\pm$ 0.1 nm (measured from high-resolution images of sections of the structure without association). The loop in the upper part of the image is shown at higher magnification in Fig. 2 *B*. The structure appears to be that of a hairpin-like turn. The loop end is composed of an approximately 200-nm-long section of HA, which is formed into a

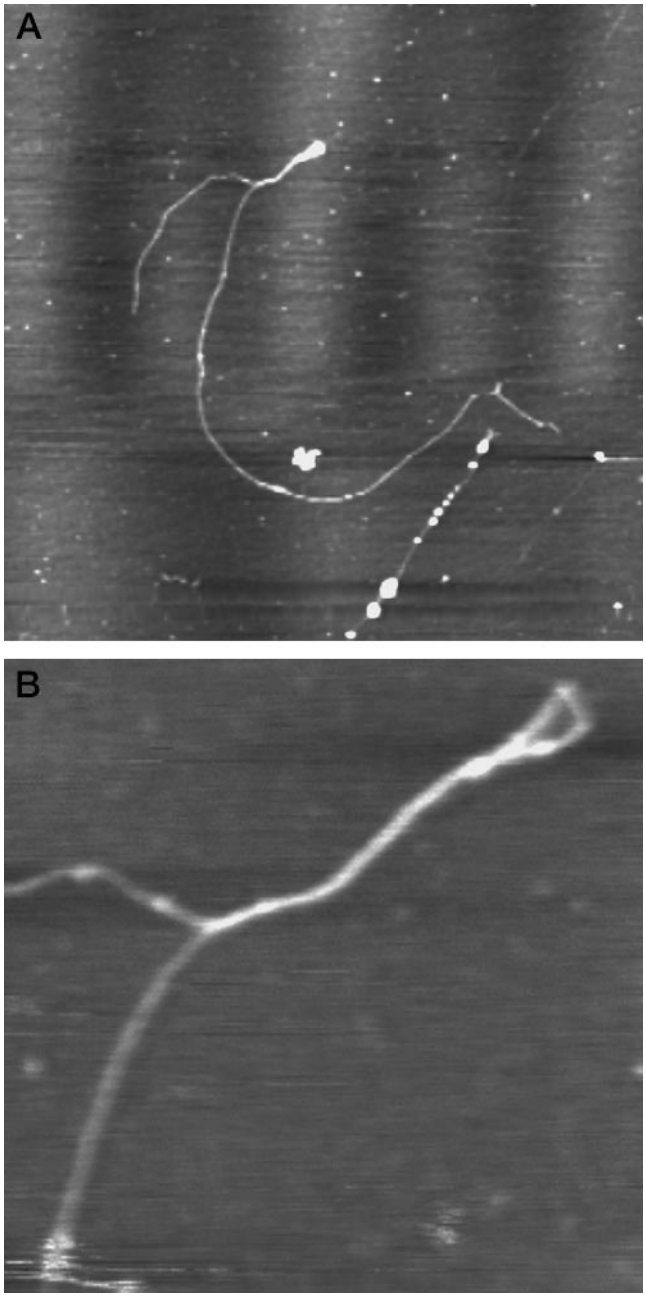

FIGURE 2 TMAFM images of an HA chain with antiparallel chain association as part of a hairpin turn structure. (*A*) Height image, 4 μm $\times$ 4 μm, with gray scale covering 2 nm in height; (*B*) Higher-magnification height image of the hairpin turn structure, 726 nm $\times$ 726 nm, with gray scale covering 3 nm.

turn and stabilized by an extended length of double-stranded self-association. The height of the structure in the double-stranded region was measured to be 1.0 $\pm$ 0.1 nm, indicating that the chain segments are not simply side by side. A double-helical arrangement of antiparallel strands is consistent with this observation.

Antiparallel chain association is also responsible for formation of a large loop (containing an approximately 600-nm segment of HA) near the end of the HA chain seen in Fig. 3 *A* and, at higher magnification, Fig. 3 *B*. One end of the chain seen in Fig. 3 *A* cannot be located in the image but appears to occur in the double-stranded stem of the loop. It is interesting to note that the HA chain in these images also crosses itself several times without forming extended associations at the junction points. The same type of simple intersection had been seen in Fig. 1. Thus, collapse of the chain on itself during the process of sample preparation does not necessarily lead to the appearance of self-association.

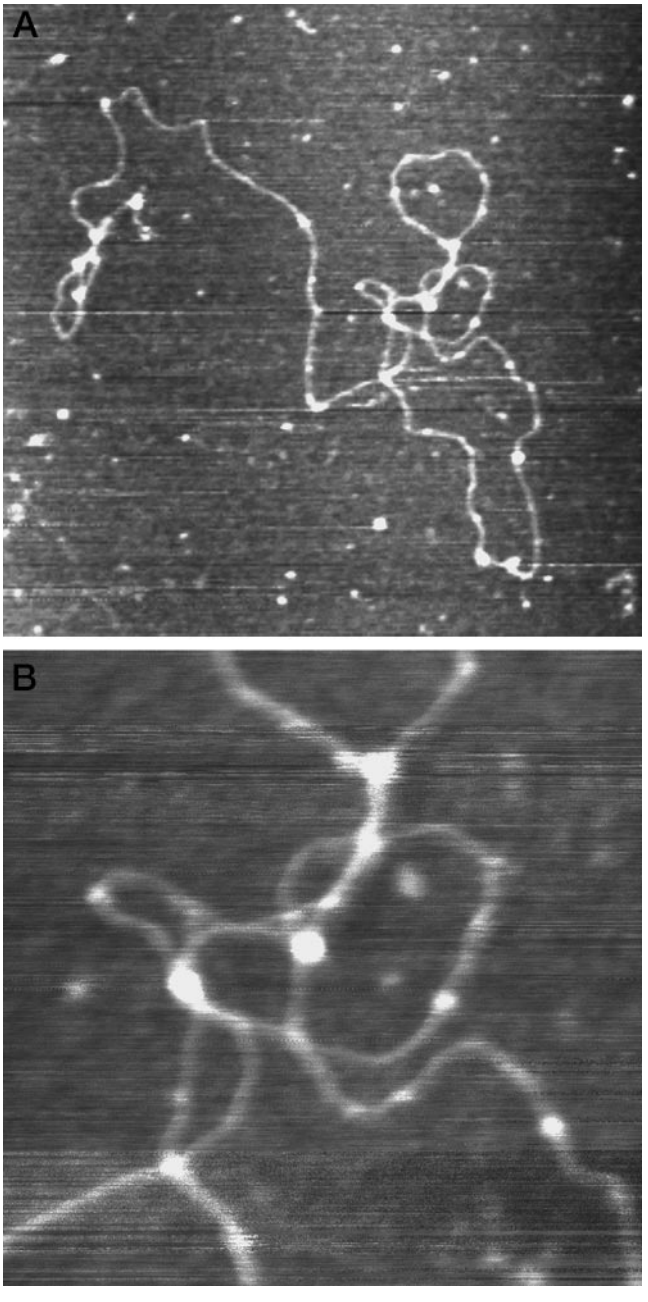

FIGURE 3 TMAFM images of an HA chain containing simple crossover points as well as antiparallel chain association in a loop structure stem. (*A*) Height image, 1.2 μm $\times$ 1.2 μm, with gray scale covering 2 nm in height; (*B*) Higher-magnification height image of the loop stem region and crossover points, 400 nm $\times$ 400 nm, gray scale covering 2 nm.

Antiparallel chain association can aid in chain direction reversal, in the formation of more compact HA structures. Fig. 4 shows a collapsed and coiled HA chain structure, with the appearance and appropriate dimensions for a stiff random coil. (The bacterial HA sample used for this image had a weight-average molecular weight of 2.2×10^6, which would be expected to have a coil diameter of ~500 nm in the low ionic strength solution applied to the mica.) The chain shows a double-stranded stem and loop at the left side of the image, which effectively reverses the chain direction abruptly.

It is not clear whether parallel associations of HA chains can also occur. Fig. 5 could represent such a structure. Only one chain end is visible. The chain could circle on itself, with an extended region of parallel association. Alternatively, the high spot at the bottom of the ring structure could be a point at which two hairpin loops, one formed near each chain end, touch each other.

More extensive self-association of HA chains is seen in Figures 6–8. In structures such as these, it becomes impossible to follow the course of the chain and to determine chain directions in associated sections. The chain segments alternately associate and separate, forming a fenestrated intramolecular matrix. It appears that the interaction junctions may contain more than two chains. Some apparent chain branches, which we observed in a number of images (see, for example, Fig. 8), are probably hairpin loops, as there is no evidence for covalent chain branches in HA.

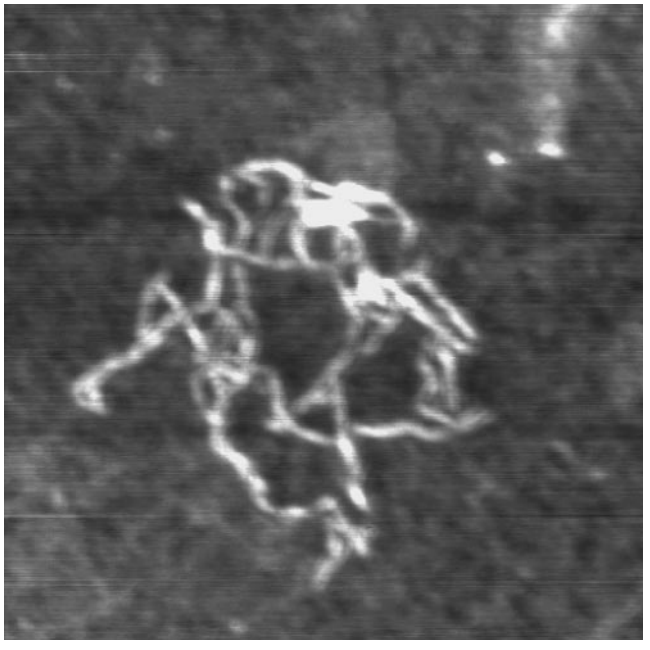

FIGURE 4 TMAFM image of a coiled HA chain in which antiparallel chain association (left side of image) leads to rapid chain direction reversal. Height image, 1 μm × 1 μm, with gray scale covering 4 nm in height.

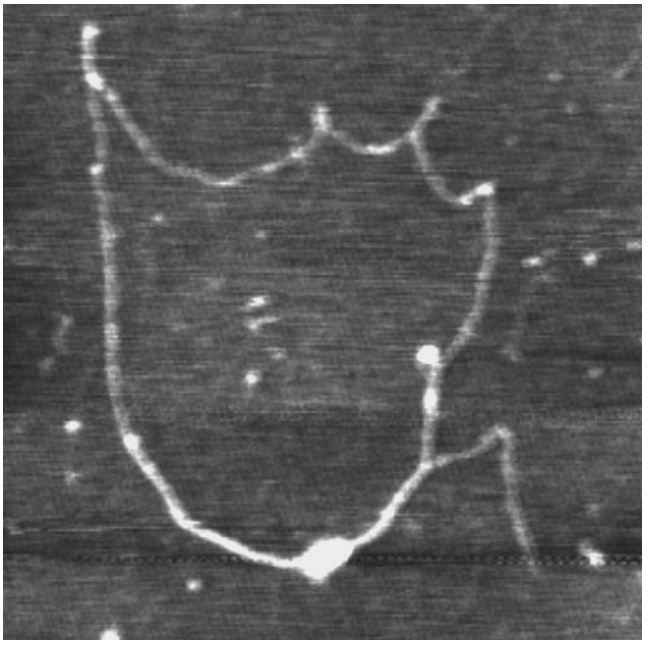

FIGURE 5 TMAFM image of HA with ambiguous polarity in self-association. A circular structure could arise from parallel association in an overlap region, or loop-to-loop association of two hairpin turn ends, each with antiparallel chain association. Height image, 1 μm × 1 μm, with gray scale covering 1.5 nm.

DISCUSSION

The present study illustrates the power of AFM, especially when used in the tapping mode, to visualize single molecules of HA. HA molecules as long as 6–7 μm have been observed in extended conformations on the mica surface. The height of a chain, corresponding to its diameter, was measured to be 0.6 ± 0.1 nm. This is in good agreement with the expected diameter of a single polysaccharide chain, based on model-building studies.

HA molecules frequently appeared in less extended structural forms as a result of intramolecular association. Wide loops and sharp hairpin-like turns were formed by antiparallel association of chain segments into stabilizing stem structures. The double-stranded stem regions were found to have a height of ~1.0 ± 0.1 nm. That height was maintained for large distances (approximately 400 nm in Fig. 2 *B*), indicating that the two chain segments must either lie one on top of the other for the entire length or, more likely, be wound about each other in a double helix. The measured height is in excellent agreement with the diameter of the HA double helix elucidated by x-ray diffraction studies (Sheehan et al., 1977; Arnott et al., 1983). The double-helical structure found by x-ray diffraction contains only antiparallel chains. Our AFM studies are not conclusive with regard to the possibility of parallel chain association, but in all cases for which chain polarity could be definitively assigned, the chains were antiparallel.

Intermittent intramolecular association of HA leads to the formation of fenestrated structures. These structures are

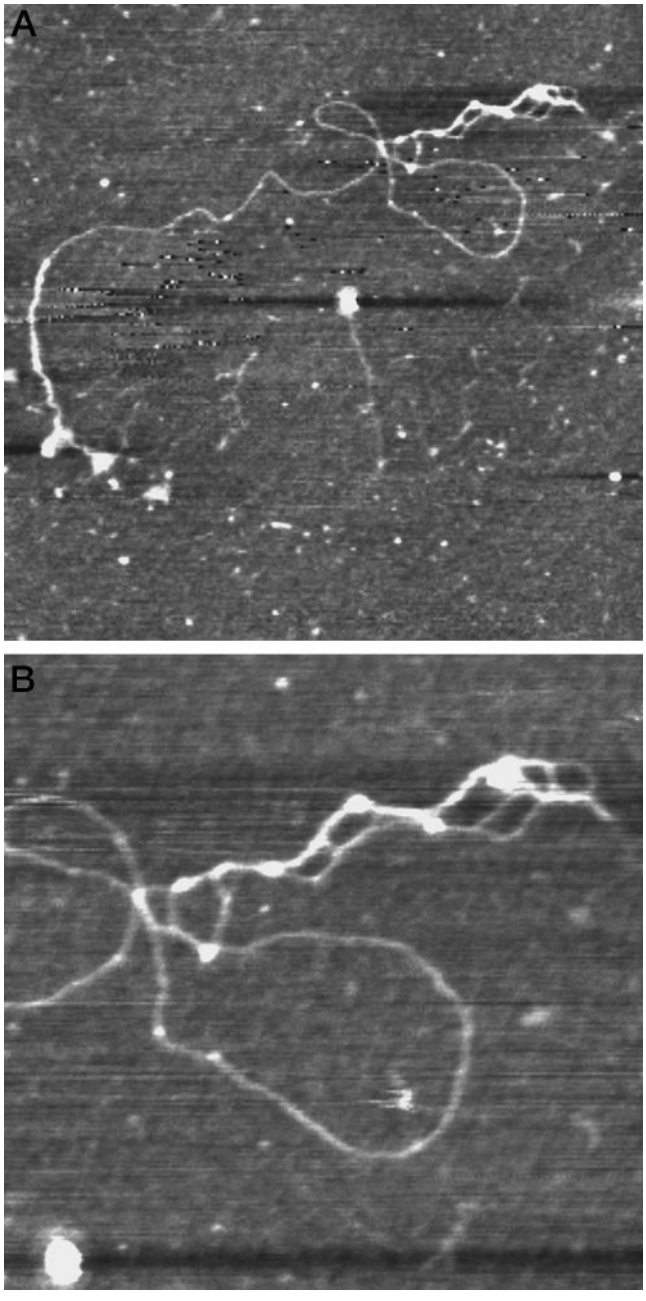

FIGURE 6 TMAFM image of an HA chain with extensive intramolecular self-association leading to a fenestrated structure. (*A*) Height image of complete chain, 1.6 μm $\times$ 1.6 μm, with gray scale covering 1.5 nm; (*B*) Higher-magnification height image showing the interacting chain segments, 700 nm $\times$ 700 nm, with gray scale covering 2 nm.

similar in appearance to the intermolecular meshworks formed at higher concentrations of HA (Scott et al., 1991; Brewton and Mayne, 1992; Cowman et al., 1998). The associated regions in some such structures may include more than two chains, the base unit of which may or may not be double helical.

HA molecules that appear to be branched structures have also been observed. The branches are proposed to be double-helical hairpin turn regions, as there is no other chemical

FIGURE 7 TMAFM image of an HA chain with extensive intramolecular self-association forming a meshwork structure. Height image, 1.5 μm $\times$ 1.5 μm, with gray scale covering 1.5 nm.

or physical evidence for branching in the covalent structure of HA.

To what extent may the structures observed by AFM reflect the physiological structure of HA? Consider the possibility that the loop and turn structures do not exist in HA when in solution but form as the polysaccharide chain

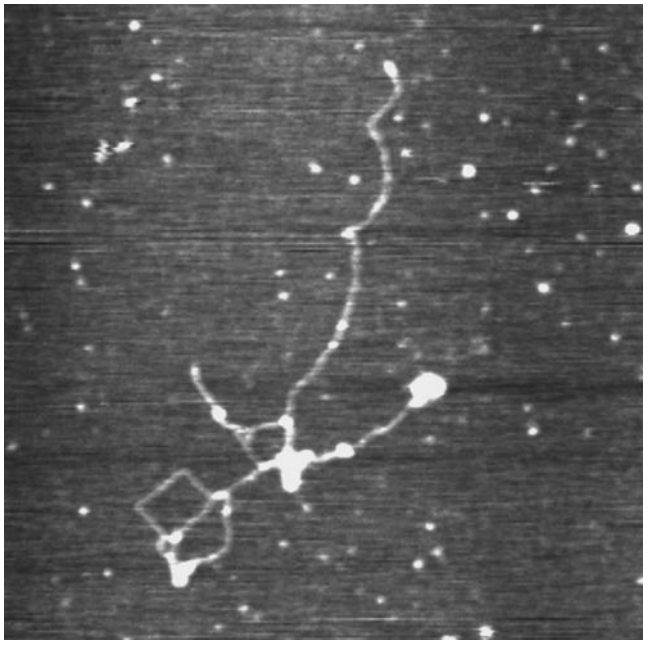

FIGURE 8 TMAFM image of an HA chain in which intramolecular self-association leads to the appearance of loops and branches. Height image, 1.5 μm $\times$ 1.5 μm, with gray scale covering 1.5 nm.

collapses on the mica surface. There are then two plausible causes for the formation of the twisted double-helical segments. The first is a simple topological constraint, similar to that seen in a long garden hose or telephone cord. If initial attachment to the surface occurs at two distant sites along the HA chain length, and if there is a twisting of the chain between the adhesion sites that cannot be easily relieved by rotation about the intervening glycosidic linkages, then the topological strain leads to the formation of twisted loops. This is analogous to the formation of supercoils in circular DNA, but in our case the circle is completed by attachment to the surface. As for DNA, the supercoils can be either positive or negative. Thus, the HA loops and turns found on the mica surface could have stems with either left-handed or right-handed twists. The HA double helix found by x-ray diffraction contains only left-handed helices. At present, our resolution is not sufficient to discern the twist sense in the double-stranded HA segments seen by AFM. It is nevertheless unlikely that this topological strain problem could explain all of the observed loops and turns observed. The chain diameter would be expected to vary along the double-stranded region if it arose from simple twisting of one chain about another without the close contacts found in the double-helix structure. Also, we have found loop structures quite near the ends of HA chains, where the possibility of topological strain is small.

A second possible cause of intramolecular associations being newly formed when the HA chains attach to the mica surface is the local high concentration of polymer chain segments and reduced water content at the surface. This possibility is supported by the observation that intermolecular interactions are prevalent in images of dehydrated HA deposited on mica from very dilute solutions (1 μg/ml) (Scott et al., 1991; Gunning et al., 1996) as well as hydrated HA deposited on mica from 100 μg/ml physiological saline solution (Cowman et al., 1998), although these HA concentrations are well below the value required for significant interpenetration of the polymeric coils. Furthermore, x-ray diffraction analysis of HA conformation and packing shows that both are sensitive to counterion type and hydration level (Sheehan and Atkins, 1983). The chain association modes and meshwork formation we have observed would, in this view, represent the tendency of HA to adopt such structures rather than their actual existence in the sample before application to the mica surface.

The final possibility to be considered is that the intramolecular loops, hairpin turn structures, and/or meshworks pre-exist in the HA sample in dilute solution. Support for this as a source for at least some of the observed structural features comes from the physicochemical analysis of HA polymer and segments in physiological solution. Thus, we had previously presented strong evidence for the formation of hairpin turn structures in HA segments containing a minimal length of ~40 disaccharides (Turner et al., 1988). Evidence for self-association of polymeric HA in physiological saline solution has also been provided by light-scattering and rheological investigations (Welsh et al., 1980; Sheehan et al., 1983).

It is likely that the form and degree of HA self-association that we have observed by TMAFM are products of both pre-existing interactions and newly formed structures. The first level of the associated HA structure is found to predominantly consist of antiparallel strands in a double-helical arrangement.

We thank Dr. Jianshe Liu, Polytechnic University, for analysis of hyaluronan molecular weight.

This research was supported by Biomatrix, Inc. This work was presented at the 1998 annual meeting of the Biophysical Society in Kansas City, MO.

REFERENCES

Arnott, S., A. K. Mitra, and S. Ragunathan. 1983. The hyaluronic acid double helix. *J. Mol. Biol.* 169:861–872.

Balazs, E. A. 1968. Viscoelastic properties of hyaluronic acid and biological lubrication. *Univ. Mich. Med. Ctr. J. (Suppl.)* 255–259.

Balazs, E. A., and J. L. Denlinger. 1985. Sodium hyaluronate and joint function. *J. Equine Vet. Sci.* 5:217–228.

Brewton, R. G., and R. Mayne. 1992. Mammalian vitreous humor contains networks of hyaluronan molecules: electron microscopic analysis using the hyaluronan-binding region (G1) of aggrecan and link protein. *Exp. Cell Res.* 198:237–249.

Cowman, M. K., J. Liu, M. Li, D. M. Hittner, and J. S. Kim. 1998. Hyaluronan interactions: self, water, ions. *In* The Chemistry, Biology, and Medical Applications of Hyaluronan and Its Derivatives. T. C. Laurent, editor. Portland Press, London. 17–24.

Fouissac, E., M. Milas, and M. Rinaudo. 1993. Shear-rate, concentration, molecular weight, and temperature viscosity dependences of hyaluronate, a wormlike polyelectrolyte. *Macromolecules*. 26:6945–6951.

Gunning, A. P., V. J. Morris, S. Al-Assaf, and G. O. Phillips. 1996. Atomic force microscopic studies of hylan and hyaluronan. *Carbohydr. Poly.* 30:1–8.

Guss, J. M., D. W. L. Hukins, P. J. C. Smith, W. T. Winter, S. Arnott, R. Moorhouse, and D. A. Rees. 1975. Hyaluronic acid: molecular conformations and interactions in two sodium salts. *J. Mol. Biol.* 95:359–384.

Laurent, T. C., U. B. G. Laurent, and J. R. Fraser. 1996. The structure and function of hyaluronan: an overview. *Immunol. Cell Biol.* 74:A1–A7.

Lee, H. G., and M. K. Cowman. 1994. An Agarose gel electrophoretic method for analysis of hyaluronan molecular weight distribution. *Anal. Biochem.* 219:278–287.

Meyer, K. 1958. Chemical structure of hyaluronic acid. *Fed. Proc. Fed. Am. Soc. Exp. Biol.* 17:1075–1077.

Morris, E. R., D. A. Rees, and E. J. Welsh. 1980. Conformation and dynamic interactions in hyaluronate solutions. *J. Mol. Biol.* 138: 383–400.

Scott, J. E., C. Cummings, A. Brass, and Y. Chen. 1991. Secondary and tertiary structures of hyaluronan in aqueous solution, investigated by rotary shadowing-electron microscopy and computer simulation. *Biochem. J.* 274:699–705.

Scott, J. E., C. Cummings, H. Greiling, H. W. Stuhlsatz, J. D. Gregory, and S. Damle. 1990. Examination of corneal proteoglycans and glycosaminoglycans by rotary shadowing and electron microscopy. *Int. J. Biol. Macromol.* 12:180–184.

Sheehan, J. K., and E. D. T. Atkins. 1983. X-ray fibre diffraction study of conformational changes in hyaluronate induced in the presence of sodium, potassium and calcium cations. *Int. J. Biol. Macromol.* 5:215–221.

Sheehan, J. K., C. Arundel, and C. F. Phelps. 1983. Effect of the cations sodium, potassium and calcium on the interaction of hyaluronate chains: a light scattering and viscometric study. *Int. J. Biol. Macromol.* 5:222–228.

Sheehan, J. K., K. H. Gardner, and E. D. T. Atkins. 1977. Hyaluronic acid: a double-helical structure in the presence of potassium at low pH and

found also with the cations ammonium, rubidium and caesium. *J. Mol. Biol.* 117:113–135.

Turner, R. E., P. Lin, and M. K. Cowman. 1988. Self-association of hyaluronate segments in aqueous NaCl solution. *Arch. Biochem. Biophys.* 265:484–495.

Welsh, E. J., D. A. Rees, E. R. Morris, and J. K. Madden. 1980. Competitive inhibition evidence for specific intermolecular interactions in hyaluronate solutions. *J. Mol. Biol.* 138:375–382.

Yanaki, T., and T. Yamaguchi. 1990. Temporary network formation of hyaluronate under a physiological condition. I. molecular-weight dependence. *Biopolymers.* 30:415–425.

Yu, L. P., J. W. Burns, A. Shiedlin, Y. Guo, T. Jankowski, P. Pradipasena, and C. Rha. 1992. Rheological characteristics of microbially derived sodium hyaluronate. *In* Harnessing Biotechnology, 21st Century, Proc. Int. Biotechnol. Symp. Expo., 9th, M. R. Ladish and A. Bose, editors. Am. Chem. Soc., Washington, D.C. 80–84.